

Inhaled Nitric Oxide Enhances Distal Lung Growth after Exposure to Hyperoxia in Neonatal Rats

YUH-JYH LIN, NEIL E. MARKHAM, VIVEK BALASUBRAMANIAM, JEN-RUEY TANG,
ANNE MAXEY, JOHN P. KINSELLA, AND STEVEN H. ABMAN

Department of Pediatrics [Y.-J.L.], National Cheng-Kung University Hospital, Tainan, Taiwan, 704, and Pediatric Heart Lung Center [N.E.M., V.B., J.-R.T., A.M., J.P.K., S.H.A.], University of Colorado Health Science Center, Denver, Colorado, 80218

ABSTRACT

Exposure of newborn rats to hyperoxia impairs alveolarization and vessel growth, causing abnormal lung structure that persists during infancy. Recent studies have shown that impaired angiogenesis due to inhibition of vascular endothelial growth factor (VEGF) signaling decreases alveolar and vessel growth in the developing lung, and that nitric oxide (NO) mediates VEGF-dependent angiogenesis. The purpose of this study was to determine whether hyperoxia causes sustained reduction of lung VEGF, VEGF receptor, or endothelial NO synthase (eNOS) expression during recovery, and whether inhaled NO improves lung structure in infant rats after neonatal exposure to hyperoxia. Newborn rat pups were randomized to hyperoxia [fraction of inspired oxygen (F_{iO_2}), 1.00] or room air exposure for 6 d, and then placed in room air with or without inhaled NO (10 ppm) for 2 wk. Rats were then killed for studies, which included measurements of body weight, lung weight, right ventricular hypertrophy (RVH), morphometric analysis of alveolarization (by mean linear intercept (MLI), radial alveolar counts (RAC), and vascular volume (Vv), and immunostaining and Western blot analysis. In comparison with controls, neonatal hyperoxia reduced body weight, increased MLI, and reduced RAC in infant rats. Lung

VEGF, VEGFR-2, and eNOS protein expression were reduced after hyperoxia. Inhaled NO treatment after hyperoxia increased body weight and improved distal lung growth, as demonstrated by increased RAC and Vv and decreased MLI. We conclude that neonatal hyperoxia reduced lung VEGF expression, which persisted during recovery in room air, and that inhaled NO restored distal lung growth in infant rats after neonatal hyperoxia. (*Pediatr Res* 58: 22–29, 2005)

Abbreviations

BPD, bronchopulmonary dysplasia
CLD, chronic lung disease
eNOS, endothelial nitric oxide synthase
MLI, mean linear intercept
NO, nitric oxide
RAC, radial alveolar counts
RVH, right ventricular hypertrophy
VEGF, vascular endothelial growth factor
VEGFR, vascular endothelial growth factor receptor
Vv, vascular volume

BPD is the chronic lung disease of infancy that follows ventilator and oxygen therapy for acute respiratory failure after premature birth (1). Traditionally, BPD has been defined by the presence of persistent respiratory signs and symptoms, the need for supplemental oxygen to treat hypoxemia, and an abnormal chest radiograph at 36 wk corrected age. Over the years, the clinical course of premature infants with BPD has changed, reflecting the effects of improved survival of babies who are less mature and have lower birth weights, as well as changes in therapeutic strategies, such as surfactant therapy

and modes of mechanical ventilation (2,3). Infants with BPD now have less severe initial acute respiratory disease, and at autopsy, lung histology is predominantly characterized by arrested lung development, including impaired alveolar and vascular growth (4).

Although mechanisms that impair lung growth in BPD are poorly understood, recent studies suggest that disruption of VEGF function plays a pivotal role in the pathogenesis of BPD. Bhatt *et al.* (5) have shown decreased lung VEGF mRNA and protein expression, as well as a reduction of the VEGF receptor, flt-1 (VEGFR-1), in the lungs of infants with fatal BPD. In addition, VEGF protein levels are reduced in the tracheal aspirates obtained from premature newborns with BPD, as well as in lung tissue from infants who died with BPD (6). Experimental studies in infant rats suggest that inhibition of VEGF receptor activity reduces alveolarization and vascular growth, resulting in histologic changes in lung structure that

Received May 20, 2004; accepted November 9, 2004.

Correspondence: Steven Abman, M.D., Pediatric Heart Lung Center, Department of Pediatrics, University of Colorado School of Medicine and The Children's Hospital, B395, 1056 E. Nineteenth Ave., Denver, CO 80218; e-mail: steven.abman@uchsc.edu.

Supported in part by grants from the National Institutes of Health (HL68702 and HL57149). Inhaled NO gas was provided by INO Therapeutics.

DOI: 10.1203/01.PDR.0000163378.94837.3E

mimic BPD (7,8). Since treatment with other anti-angiogenesis agents, thalidomide and fumagillin, also inhibits alveolarization and reduces vascular density (7), it has been hypothesized that injury to the developing pulmonary circulation after premature birth can disrupt normal lung angiogenesis, perhaps through impaired VEGF signaling, and may contribute to abnormal lung growth in BPD (4,7–9).

Prolonged exposure of neonatal rats to hyperoxia causes several structural changes in the lung that are similar to lung histology from human infants with BPD, such as decreased alveolar septation, increased terminal air space size, and dysmorphic vascular growth (10–12). Although hyperoxia has been implicated in the pathogenesis of BPD, the exact mechanisms by which increased oxygen tension inhibits lung growth and alters lung structure in BPD are uncertain. Past studies have demonstrated that acute hyperoxia decreases VEGF mRNA and protein expression, suggesting that hyperoxia-induced down-regulation of VEGF may contribute to abnormal lung structure in this model (13,14). Decreased lung VEGF and VEGF receptor expression has also been found in the primate model of CLD (15). Thus, impaired VEGF signaling has been demonstrated in animal models of BPD, as well as in human infants with BPD, but mechanisms through which decreased VEGF expression contributes to BPD are uncertain.

Several studies have shown that VEGF increases the expression of eNOS mRNA and protein, and acutely stimulates NO release through activation of VEGFR-2 *in vitro* (16–18). NO production has also been shown to mediate the angiogenic effects of VEGF in the systemic circulation *in vivo* (16,17). Recently, mice with a genetic deficiency of eNOS expression were shown to have impaired vascular and alveolar growth *in utero*, and have increased susceptibility for impaired lung growth during postnatal hypoxia (19,20). Whether NO mediates VEGF-induced angiogenesis in the developing lung and whether decreased NO production contributes to abnormal lung structure in BPD are unknown.

Past studies have examined the roles of inhaled NO treatment in several animal models of acute lung injury, including hyperoxia exposure. Inhaled NO administered with high concentrations of oxygen has been shown to improve survival and protect the lung endothelium and the alveolar epithelium against O₂-mediated injury (21–24). In past studies of inhaled NO treatment of hyperoxia-induced lung injury, NO was delivered during the exposure to hyperoxia, and there are no data on the long-term effects on lung structure. The effects of inhaled NO treatment after the hyperoxia exposure period and its effects on lung structure during the critical period of postnatal alveolarization are unknown.

Therefore, we hypothesized that inhaled NO therapy after hyperoxia exposure may enhance the recovery of lung growth and structure during infancy. To address this question, we first studied the effects of neonatal hyperoxia on lung VEGF, VEGF receptor, and eNOS expression in the developing lung during recovery in room air. We further studied the effects of prolonged, low-dose treatment with inhaled NO during recovery on lung structure and VEGF expression. We report that neonatal hyperoxia down-regulated lung VEGF, VEGFR-2, and eNOS expression, and that late treatment with inhaled NO improved alveolarization during infancy, without increasing VEGF expression.

METHODS

Animals. All procedures and protocols were approved by the Animal Care and Use Committee at the University of Colorado Health Sciences Center. Pregnant Sprague-Dawley rats (SDR) were purchased (Harlan Laboratories, Indianapolis, IN) and maintained at Denver's altitude [1,600 m; barometric pressure (PB), 630 mm Hg; inspired oxygen pressure (P_IO₂), 122 mm Hg] for at least 1 wk before giving birth. Pups were delivered naturally (on d 21) and the litter size was maintained at 11–12 pups. Animals were fed *ad libitum* and exposed to day-night cycles alternatively every 12 h throughout the study period.

Study design. Four groups of animals were used in these experiments. All pups were maintained in room air for the first 24 h to allow successful transition to postnatal life after birth, before random assignment to four study groups. These study groups included the following treatments: neonatal rats exposed to hyperoxia (>95% oxygen at Denver's altitude) for 6 d and maintained in room air for 2 wk (hyperoxia–room air, the HR group); neonatal rats maintained in hyperoxia for 6 d and then treated with inhaled nitric oxide (NO, 10 ppm) for 2 wk (hyperoxia–NO, the HN group); neonatal rats maintained in room air throughout the 20-d experimental period (room air–room air, the RR group); and neonatal rats maintained in room air for 6 d and then treated with inhaled NO (10 ppm) for 2 wk (room air–NO, the RN group). Litters of randomly divided rat pups and their dams were placed in Plexiglas chambers containing >95% O₂ or room air. Oxygen concentrations were monitored continuously, and gas lines were filtered with charcoal and barium hydroxide to maintain CO₂ levels below 0.05%. Chambers were opened briefly (less than 10–15 min) for cleaning or switching dams. Dams were rotated during the hyperoxia exposure due to poor tolerance of adult rats to hyperoxia. Inhaled NO was delivered and NO and NO₂ levels were continuously monitored with an INO Vent (INO Therapeutics, Clinton, NJ). During (d 7 and 14) and at the end of the study (d 21), animals were killed with an intraperitoneal injection of pentobarbital sodium (0.3 mg/g body wt), and formalin-fixed lung tissue was obtained for histology and morphometric analysis.

RVH. At autopsy, the heart was resected through a midline sternotomy. The right ventricle (RV) and left ventricle plus septum (LV+S) were dissected and weighed, and the ratio of RV to LV+S weights were determined as standard assessments of RVH.

Fixation of lung tissue. Rat lungs were prepared and fixed *in situ* at the end of the study (d 21). PBS was first infused through a main pulmonary artery catheter to flush the pulmonary circulation free of blood. The lungs were then fixed by tracheal installation of 10% buffered formalin at constant pressure (20 cm H₂O). The trachea was ligated under pressure after sustained inflation for 15 min. The lungs were removed and submerged in fixative for 24 h at 4°C.

Lung morphometric analysis. Transverse sections were obtained from the midplane of the upper, middle, and lower lobes of the formalin-fixed right lung for morphometric analysis. Sections from each animal were processed and embedded in paraffin wax. Paraffin sections (5 μm thick) were cut from each block and stained with hematoxylin and eosin. Analysis of each section was carried out in a blinded fashion. Alveolarization was assessed by performing RAC, according to the method of Emery and Mithal (25,26). Respiratory bronchioles were identified as bronchioles lined by epithelium in one part of the wall. From the center of the respiratory bronchiole, a perpendicular line was drawn to the edge of the acinus (as defined by a connective tissue septum or the pleura), and the number of septa intersected by this line was counted. Ten counts were performed for each animal.

For assessment of the MLI, five lung sections were selected in an unbiased fashion. Images of each section were captured with a ProgRes 3008 digital camera through a Zeiss Axioskop2 microscope, and were saved as PICT files. The images were then analyzed with the use of Stereology Toolbox software (Morphometrix, Davis, CA). The mean interalveolar distance, or distance between airspace walls, was measured as the MLI, by dividing the total length of lines drawn across the lung section by the number of intercepts encountered, as described by Cooney and Thurlbeck (25,26).

Vessel wall thickness measurements were performed by an observer blinded to the identity of the histology slides. Wall thickness measurements were performed on small pulmonary arteries (20–60 μm) associated with terminal bronchioles and distal air spaces with a Zeiss Interactive Digital Analysis System (ZIDAS; Carl Zeiss Inc., Thornwood, NY). Wall thickness and external diameter were measured directly and expressed as the percentage of wall thickness, which was calculated with the following formula: [(external diameter – internal diameter)/external diameter] × 100 (27).

Immunohistochemistry and vessel volume density. Immunohistochemistry for factor VIII was performed to assess vascular density. Paraffin-embedded slides from formalin-fixed tissue were deparaffinized in CitriSolv (Fisher Scientific, Pittsburgh, PA). The sections were rehydrated by serial immersions in 100% ethanol, 95% ethanol, 70% ethanol, and water. Sections were digested with proteinase K at a concentration of 500 g/mL for 10 min at room

temperature and then washed with PBS with 2.7 mM KCl, 1.2 mM KH_2PO_4 , 138 mM NaCl, and 8.1 mM Na_2HPO_4 . Endogenous peroxidase activity was reduced by immersion in 3% hydrogen peroxide in methanol. After rinsing, sections were covered in 10% goat serum for 30 min and incubated with rabbit anti-factor VIII antibody (1:1000) diluted in PBS with 1% BSA and 0.1% sodium azide for 60 min. After incubation, the sections were rinsed with PBS and incubated with biotin-labeled secondary antibody diluted 1:200 in PBS with 2% goat serum for 30 min. After incubation with the secondary antibody, the sections were rinsed with PBS, incubated in ABC complex (Vector Laboratories, Burlingame, CA) for 30 min at room temperature, rinsed in PBS and developed with diaminobenzidine (DAB) and hydrogen peroxide. Slides were lightly counterstained with hematoxylin. The slides were then dehydrated by sequential immersion in 70% ethanol, 95% ethanol, 100% ethanol, and CitriSolv before applying coverslips. Immunostaining for eNOS and VEGF protein were also performed by similar methods.

Five lung sections were selected and captured by digital camera for analysis. A point-counting method, in which the lung parenchymal tissue served as the volume of reference, was used to determine the volume fraction (Vv) of factor VIII immunoreactive sites. A grid of 100 points is superimposed on color photographs captured by digital camera at a magnification of 100 \times . The number of points falling on immunoreactive sites and on lung parenchyma was recorded. The Vv (positive stained profile/parenchyma) was calculated as the ratio of the number of points falling on factor VIII immunoreactive sites to points on lung parenchyma.

Western blot analysis. We performed Western blot analysis of distal lung homogenates from HR, HN, and RR study groups on d 7 and 14. Western blot analysis was performed according to previously published techniques (9) with the following primary antibodies: a MAb to eNOS (Transduction Laboratories, Lexington, KY), VEGF [VEGF (A-20), Santa Cruz Biotechnology, Santa Cruz, CA], VEGFR-2 (KDR, Santa Cruz Biotechnology), VEGFR-1 (FLT-1, Santa Cruz Biotechnology), PECAM (Santa Cruz Biotechnology). Lung tissue was homogenized on ice in 25 mM Tris · HCl, pH 7.4, containing 1 mM EDTA, 1 mM EGTA, 0.1% (vol/vol) 2-mercaptoethanol, 1 mM phenylmethylsulfonyl fluoride, 2 mM leupeptin, and 1 mM pepstatin A. Samples were centrifuged at 1500 \times g at 4°C for 10 min to remove cell debris. Lung homogenates (25 g) were separated by SDS-PAGE and then transferred to nitrocellulose membranes by electroblotting. Blots were blocked overnight at 4°C in 50 mM Tris · HCl, pH 7.4, 150 mM NaCl, 2% (vol/vol) BSA, and 0.1% (vol/vol) Tween 20, and then incubated with the primary antibody for 1 h at room temperature. Primary antibody was diluted 1:500 in blocking buffer. Blots were then washed six times for 5 min per wash with 50 mM Tris · HCl, pH 7.4, 150 mM NaCl, and 0.1% (vol/vol) Tween 20 at room temperature to remove unbound antibody, incubated for 1 h with anti-mouse IgG antibody coupled to horseradish peroxidase diluted in blocking buffer, and then washed again with Tris-buffered saline-Tween 20 at room temperature. Protein bands were detected by chemiluminescence after exposure to x-ray film (ECL Plus detection, Amersham Pharmacia Biotech, Inc., Piscataway, NJ). Densitometry was performed with a scanner and NIH Image software (National Institutes of Health, Bethesda, MD). We initially determined the accuracy and consistency of the protein loads for each gel by Ponceau S staining before applying the different antibodies. In addition, each gel was stripped and reprobed with β -actin for use as a housekeeping protein to compare expression between samples. The experiments were performed with at least five animals per study group, and data represents at least three different experiments.

To assess isoform specificity of the antibody to VEGF, a Western blot analysis was performed using recombinant human VEGF 165 (rhVEGF) protein, in which rhVEGF was preincubated with the antibody to VEGF used in our studies. We found that the rhVEGF protein band migrated with the VEGF band identified from tissue homogenate from rat lung, and that preincubation of the blocking peptide with VEGF antibody eliminated the VEGF bands. These findings suggest that the predominant isoform measured by Western blot analysis is VEGF 164 (data not shown). Statistical Analysis

Statistical comparison was made using analysis of variance and Fisher's protected least significant difference test with StatView software (Abacus Concepts, Berkeley, CA). Differences were considered significant at $p < 0.05$. The results were presented as mean \pm SD.

RESULTS

Body and lung weights, RVH, and pulmonary vascular remodeling. Mortality was not different between study groups. The number of animals within each study group included 18 pups in the HR group, 23 in the HN group, 20 in the RR group, and 20 in the RN group. In comparison with room air controls (RR), hyperoxia caused a significant reduction in body weight (33 ± 7 g versus 41 ± 3 g, for HR and RR, respectively; $p < 0.05$) (Table 1). Inhaled NO treatment after rats were exposed to hyperoxia (HN) increased body weight toward room air (RR) control values (44 ± 7 g, $p > 0.05$ for HN versus RR) (Table 1). Inhaled NO treatment of control rats with prior room air exposure (RN) did not change body weight when compared with room air (RR) control animals (44 ± 2 g; $p = \text{NS}$ for RN versus RR) (Table 1). Lung weight to body weight ratios in control room air control (RR) animals (0.016 ± 0.001) was greater than rats that were exposed to hyperoxia (0.014 ± 0.001 for HR; $p < 0.05$ for RR versus HR), and not different from HN animals (Table 1). Measurements of RVH and vessel wall thickness of small pulmonary arteries were not different between any of the study groups (Table 1).

Lung histology and morphometric analysis. In comparison with control animals (RR), lung histology from hyperoxia-treated rats (HR) was characterized by decreased septation, and the appearance of a widened distal airspace (Fig. 1). In comparison with hyperoxia-exposed rats that remained in room air during recovery (HR), inhaled NO therapy improved distal lung structure, as reflected by smaller and more numerous alveoli (HN; Fig. 1). To quantitate these differences, morphometric analysis of RAC and MLI were compared between study groups (Fig. 2). As shown, RAC was decreased in hyperoxia-exposed rats that were recovered in room air (8.2 ± 1.6 , HR versus 11.5 ± 1.8 , RR; $p < 0.05$). Inhaled NO after hyperoxia (HN) increased RAC in comparison with room air recovery rats (HR), and was not different from RR control animals. RAC in rats that were treated with inhaled NO without hyperoxia exposure (RN) were not different from room air (RR) controls.

Measurements of MLI were greater in the HR group when compared with RR control values (55 ± 9 , HR versus 45 ± 7 μm , RR; $p < 0.05$). Inhaled NO treatment after hyperoxia (HN) reduced MLI from HR rats and was not different from

Table 1. Body and lung weights and lung morphometric analysis

	HR	HN	RR	RN	<i>p</i> value
Body Weight	$33 \pm 7^*$	44 ± 7	41 ± 3	44 ± 2	<0.05
Lung wt/BW	$0.014 \pm 0.001^*$	$0.014 \pm 0.001^*$	0.016 ± 0.001	$0.015 \pm 0.002^*$	<0.05
RV/(LV+S)	0.35 ± 0.05	0.35 ± 0.07	0.37 ± 0.04	0.32 ± 0.02	NS
MLI	$55 \pm 9^*$	45 ± 6	45 ± 7	39 ± 2	<0.05
RAC	$8.2 \pm 1.6^*$	10.3 ± 1.3	11.5 ± 1.8	11 ± 3	<0.05
Vv	0.27 ± 0.18	0.36 ± 0.28	0.20 ± 0.08	$0.22 \pm 0.11^*$	<0.05

Abbreviations: wt, weight; BW, body weight; Lung wt/BW, lung weight to body weight ratio; MLI, mean linear intercept; RAC, radial alveolar count; RV/LV+S, ratio of right ventricle to left ventricle plus septum weights; Vv, vascular volume.

* Comparison with RR group. ($N = 18$ pups for HR; 23 pups for NH; 20 for RR; and 20 for RN).

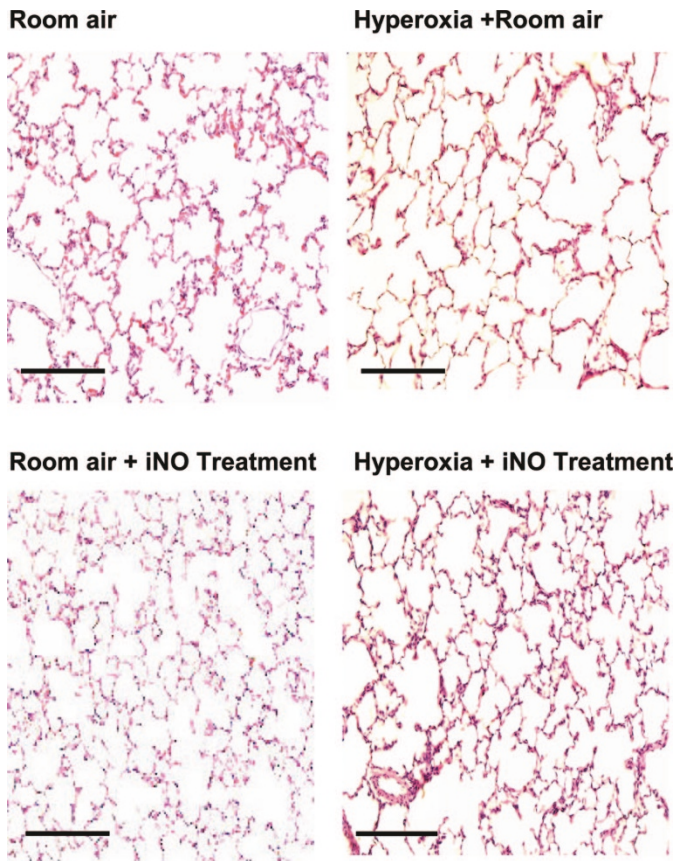


Figure 1. Lung histology from infant rats after recovery from hyperoxia in room air or after inhaled NO therapy (10 ppm). In comparison with room air controls (*upper left panel*), neonatal hyperoxia exposure with recovery in room air reduced alveolarization (*upper right panel*). Inhaled NO therapy after hyperoxia improved distal lung structure (*lower left panel*). Inhaled NO in room air controls did not appear to affect lung structure (*lower right panel*). Bar length = 100 μm .

RR and RN groups (Fig. 2, *lower panel*). In addition to the morphometric assessment of alveolarization, measurements of vessel volume density (Vv) demonstrated increased Vv in the HN group in comparison with the other study groups (Fig. 3).

Western blot analysis. To determine the effects of hyperoxia on VEGF-NO signaling, and changes in the VEGF-NO cascade during recovery after hyperoxia, four animals from HR, HN, and RR groups were killed on d 7 and 14 to obtain lung tissue for Western blot analysis of VEGF (Fig. 4), VEGF receptors (VEGFR-1 and VEGFR-2, Fig. 5), eNOS (Fig. 8), and PECAM, an endothelial cell marker. As shown, neonatal exposure to hyperoxia down-regulated lung VEGF expression, as demonstrated by the decrease in lung VEGF protein content in HR and HN rats *versus* RR controls (Fig. 4). Importantly, lung VEGF expression remained decreased even after termination of the hyperoxia exposure, as demonstrated by the persistent reduction in lung VEGF content in HR rats in comparison with room air controls (RR). Although inhaled NO improved lung structure, NO treatment after neonatal hyperoxia did not increase VEGF expression. Hyperoxia also initially decreased VEGFR-2 expression at d 7, but levels were not different from controls at d 14 (Fig. 5). There were no differences in lung VEGFR-1 content expression on d 7 and 14 between the study groups (data not shown). As observed with

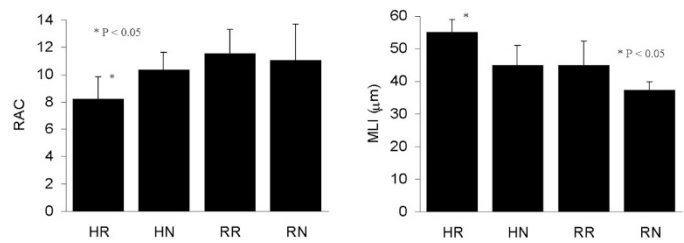


Figure 2. Morphometric analysis of alveolarization from infant rat lungs after exposure to hyperoxia followed by placement in room air or inhaled NO. As shown, infant rats that were exposed to neonatal hyperoxia and were recovered for 2 wk in room air (HR) had lower RAC (*upper panel*) and higher MLI (*lower panel*) than room air controls (RR, $p < 0.05$ for each comparison). Inhaled NO treatment after hyperoxia (HN) increased RAC and decreased MLI in comparison with room air recovery (HR, $p < 0.05$). RAC and MLI values in neonatal rats that were treated with inhaled NO without hyperoxia exposure (RN) were not different from controls. $n = 6-8$ pups per study group.

VEGFR-2 expression, hyperoxia also decreased lung eNOS protein at d 7, but levels were not different from control animals during the recovery period (d 14) (Fig. 6). In contrast, lung PECAM protein content was not different between study groups after hyperoxia or during the recovery period.

Immunostaining. Figures 7 and 8 illustrate the sites of expression for VEGF and eNOS expression, respectively, in the different study groups at d 21. As shown, lung VEGF is predominantly expressed in the airway epithelium and appears decreased after recovery from hyperoxia (Fig. 7). Lung eNOS protein is primarily present in vascular endothelium in each group (Fig. 8).

DISCUSSION

We found that hyperoxia exposure of neonatal rats impairs distal lung growth, as demonstrated by reduced alveolarization and Vv, and that these changes in lung structure are present despite prolonged recovery in room air. We further report that hyperoxia down-regulates lung VEGF protein expression in the neonatal lung, and that this reduction in VEGF protein persists during infancy despite recovery in room air. In addition, lung VEGFR-2 and eNOS expression, but not lung VEGFR-1 and

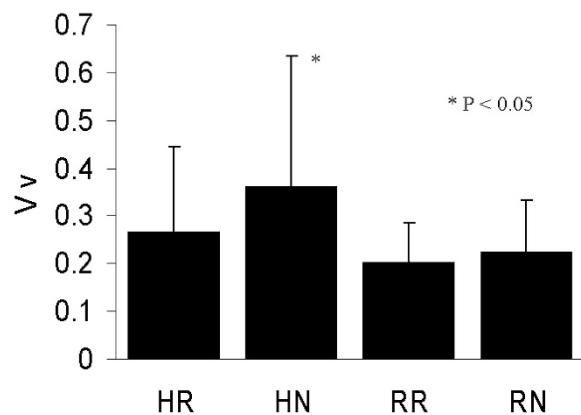


Figure 3. Vv measurements in infant rats after neonatal hyperoxia, with recovery in room air (HR) or inhaled NO treatment (HN) or control rats (RR). As shown, treatment with inhaled NO increased Vv in comparison with hyperoxia-exposed rats that were recovered in room air ($p < 0.01$, HN vs HR).

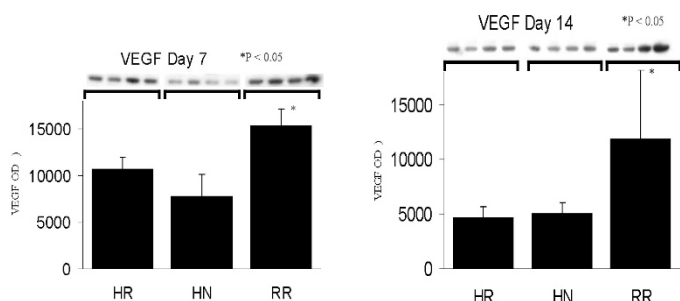


Figure 4. Lung VEGF protein content in control (RR), hyperoxia (HR), and hyperoxia plus NO (HN) study groups as quantified by Western blot analysis. As shown, hyperoxia reduced lung VEGF protein content in comparison with room air controls at d 7 and 14 (HR and HN vs RR at d 7 and 14, respectively; $p < 0.01$ and $p < 0.05$). Inhaled NO during recovery after hyperoxia did not alter lung VEGF protein content in comparison with room air recovery (HN vs HR groups, $p = \text{NS}$). $n = 5\text{--}8$ pups per study group.

PECAM expression, are reduced during neonatal hyperoxia. In contrast with the sustained decrease of VEGF expression, however, lung VEGFR-2 and eNOS protein return to control values during the recovery period after hyperoxia. Furthermore, we demonstrate that late treatment with low doses of inhaled NO (10 ppm) during the recovery period improves lung architecture, as demonstrated by increased RAC, decreased MLI, and increased Vv.

Overall, these findings provide further support to the hypothesis that inhibition of alveolarization following neonatal hyperoxia may be partly due to sustained impairment of VEGF signaling, which persists during infancy despite recovery in room air. Because late treatment with NO improves alveolarization, we further speculate that the effects of hyperoxia on distal lung growth may at least partly be due to impaired VEGF-NO signaling, and that prolonged treatment with inhaled NO may enhance distal lung growth in this model of BPD. Past studies have shown that pharmacologic inhibition of VEGF receptors in neonatal rats impairs alveolarization in older rats (7,8) and is associated with decreased lung eNOS protein content and NO production (28,30). As observed in this post-hyperoxia model, treatment with inhaled NO also improved alveolarization after inhibition of VEGF activity (28). These experimental findings are especially interesting due to recent clinical studies that have demonstrated decreased VEGF expression in lung tissue and bronchoalveolar lavage fluid of human infants with BPD (6). In addition, a recent single-center study has suggested that acute inhaled NO treatment of premature infants with BPD reduces the incidence of chronic lung disease and death in human newborns (18).

Exposure of neonatal rats to hyperoxia has provided a useful experimental model to study mechanisms that contribute to the development of BPD (10–12). Although hyperoxia is likely to inhibit lung growth through diverse mechanisms, recent clinical and laboratory studies have suggested that impaired VEGF signaling may play a prominent role in the pathogenesis of BPD. First, lung VEGF and VEGF receptor expression are reduced in human infants who died with severe BPD, and tracheal fluid VEGF levels are lower in samples from premature neonates with BPD than controls (5,6). Second, animal studies have previously shown that hyperoxia acutely reduces

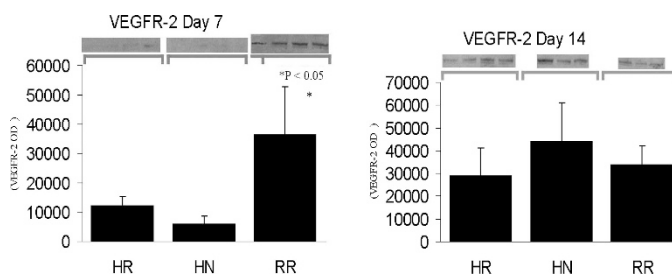


Figure 5. Lung VEGFR-2 protein expression in control (RR), hyperoxia (HR), and hyperoxia plus NO (HN) study groups as assessed by Western blot analysis. Hyperoxia reduced lung VEGFR-2 protein content in comparison with room air controls at d 7 (RR vs HN and HR, $p < 0.01$). During recovery at d 14, lung VEGFR-2 protein content was not different between study groups. $n = 6\text{--}8$ pups per study group.

lung VEGF expression in neonatal rabbits within the initial 48 h of exposure (30). In contrast with past work suggesting that VEGF increases during the recovery period following hyperoxia (14), we report sustained reduction of lung VEGF expression, suggesting that the late structural abnormalities may be associated with continued impairment of VEGF signaling. These findings further extend a recent study of hyperoxia in neonatal rats, which showed sustained reduction of lung VEGF and VEGFR-2 expression during prolonged hyperoxia, but did not measure lung VEGF expression during recovery after hyperoxia (31). Third, treatment of neonatal rats with SU5416, a VEGF receptor inhibitor, reduced alveolarization and lung to body weight ratio, providing direct evidence that impairment of VEGF signaling inhibits lung growth (7,8). Thus, it is likely that persistent reduction of VEGF expression after hyperoxia alters angiogenesis and impairs alveolarization in the hyperoxia model of BPD. Mechanisms underlying sustained decreases in VEGF expression are unknown, but may be related to suppression of hypoxia-inducible factor 2- α expression (32).

Because NO has been shown to mediate many of the pro-angiogenic effects of VEGF, we hypothesized that neonatal hyperoxia would cause sustained reduction in lung VEGF and eNOS expression, and that treatment with inhaled NO may augment lung growth after hyperoxic injury. That hyperoxia reduces lung VEGF expression has been previously reported (13,30,31), but these findings extend past observations by showing that lung VEGFR-2 and eNOS are also down-regulated after hyperoxia. In addition, lung VEGF protein remains decreased despite termination of hyperoxia exposure, suggesting that sustained reductions of VEGF may limit lung growth during the recovery period in infant rats. Inasmuch as lung PECAM and VEGFR-1 protein expression do not change during hyperoxia, these findings suggest that hyperoxia has a relatively selective effect on endothelial expression of VEGFR-2 and eNOS, rather than a more generalized impairment of endothelial cell function. Interestingly, NO may contribute to branching morphogenesis in fetal rat lungs *in vitro* and to compensatory lung growth in rats after pneumonectomy *in vivo* (20,32,33). In addition, neonatal mice with eNOS insufficiency have an increased susceptibility to impaired vascular growth and alveolarization in response to mild hypoxia

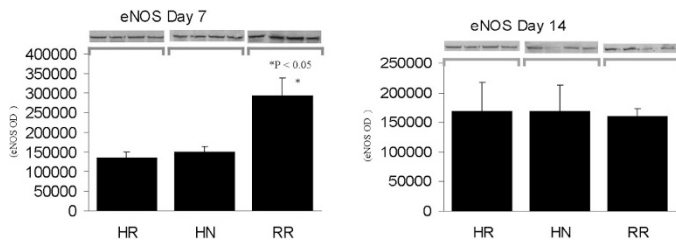


Figure 6. Lung eNOS protein expression in control (RR), hyperoxia (HR), and hyperoxia plus NO (HN) study groups as assessed by Western blot analysis. Hyperoxia reduced lung eNOS protein content in comparison with room air controls at d 7 (RR vs HR and HN, $p < 0.05$). During recovery at d 14, lung eNOS protein content was not different between study groups. $n = 5$ –8 pups per study group.

(20). Recent studies have also found that lung eNOS expression is decreased in primate and lamb models of BPD, further suggesting that impaired NO production may contribute to the pathogenesis of BPD (34,35).

Previous studies have demonstrated that inhaled NO during hyperoxia exposure may reduce acute lung injury in several animal studies (23,24,36–38), but some studies have shown opposing results (39–43). In these latter studies, however, inhaled NO was administered with high fraction of inspired oxygen (F_{iO_2}) and may have resulted in enhanced exposure to NO_2 and peroxynitrite, which may have some detrimental effects on the lung. In our study, inhaled NO treatment followed neonatal exposure to hyperoxia, which would decrease the potential harmful effects of NO_2 and peroxynitrite.

Although the exact mechanism by which late inhaled NO treatment enhances distal lung growth is unclear, we found that VEGF expression is decreased in hyperoxia-exposed pups. Prolonged exposure of a neonatal animal to hyperoxia creates a lesion that is similar to human BPD (11). Animal models have also showed the adverse effects of prolonged hyperoxia on the developing pulmonary circulation. Endothelial cells are especially prone to oxidant injury, and the absence of VEGF, an important endothelial cell survival factor, may further increase susceptibility of the endothelium to hyperoxic injury (43). NO plays an integral role in VEGF signaling, not only by modulating vasorelaxation and permeability but also by playing an important role in the angiogenesis *in vitro* and *in vivo* (44). NO is involved in endothelial cell proliferation and migration, which are essential for angiogenesis (17). By using the human umbilical vein endothelial cells (HUVEC), Papatropoulos *et al.* (17) reported that VEGF treatment increases eNOS expression and stimulates NO release through activation of VEGFR-2 and PI-3kinase/Akt signaling. NO is a downstream molecule that mediates VEGF-induced endothelial cell proliferation, migration, and organization (17). Thus, decreased VEGF expression likely reduces endothelial cell function, growth, survival, and NO production. Whether reduced NO production contributes to impaired alveolarization after neonatal hyperoxia is uncertain, but the effects of low-dose inhaled NO in enhancing distal vascular and alveolar growth supports this hypothesis. Similarly, reduced NO production impairs alveolar growth in response to mild hypoxia, further suggesting a role for NO in lung development (20).

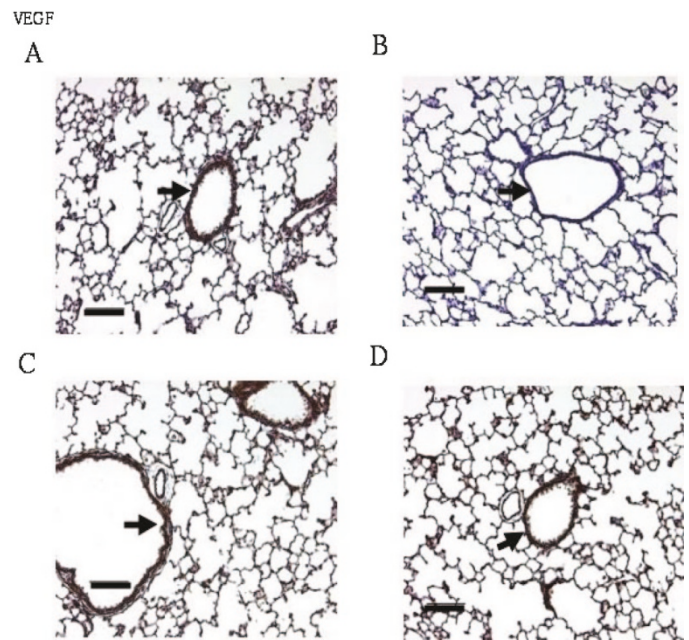


Figure 7. Immunolocalization of VEGF protein in room air controls (RR, A), neonatal hyperoxia with room air (HR, B) or inhaled NO (HN, C) recovery, and room air rats with NO treatment (RN, D). As shown, VEGF is primarily expressed in the airway epithelium (arrow) for each study group. In comparison with RR and HN, VEGF intensity appears less in the HR group. Bar length = 100 μ m.

There are several potential limitations in our study, which include the use of term rather than premature neonatal rats as an animal model of BPD. Although there are clear maturational differences between the premature and term lung, alveolarization in the newborn rat occurs within the first 2 wk of postnatal life, thereby providing a useful window for studying basic mechanisms that can impair lung development (44–46). Inasmuch as host antioxidant defense mechanisms are less developed in preterm than term rats, it is likely that exposure to similar levels of

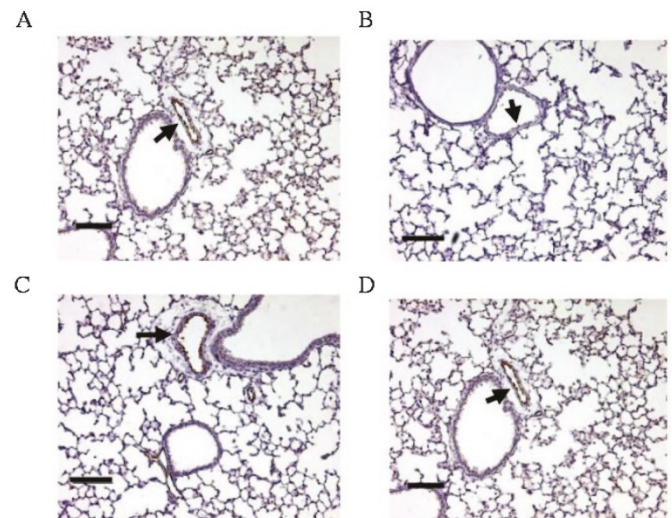


Figure 8. Immunolocalization of eNOS protein in room air controls (RR, A), neonatal hyperoxia with room air (HR, B) or inhaled NO (HN, C) recovery, and room air rats with NO treatment (RN, D). Lung eNOS is primarily expressed in vascular endothelium (arrows) for each study group. Bar length = 100 μ m.

hyperoxia after birth would have more adverse effects on lung growth and survival (46,47). Although it has been shown that the preterm rats were not more susceptible to O₂-induced lung damage and lethality than full-term newborns (46,47), it is also possible that inhaled NO would not have had similar effects on preterm rats as observed in this study of term neonatal rats. We exposed our neonatal rats to 95% oxygen for 6 d, which can cause higher mortality and more severe signs of lung inflammation and fibroproliferative changes on lung histology (48,49). At Denver's altitude, this level of hyperoxia would be more similar to exposure of 75–80% Fio₂ at sea level. This likely accounts for less severe acute lung injury in our study, but still provides a model of impaired lung development, which more closely mimics the “new BPD” in the postsurfactant era (3,4). Past studies have examined the combined effects of inhaled NO treatment during acute exposure to hyperoxia (21–24,48,49). In contrast, we have examined the effects of late NO treatment after hyperoxia exposure to more directly examine its effects during recovery from acute lung injury. Whether prolonged inhaled NO during acute hyperoxia with or without late treatment would have similar effects is uncertain.

In summary, we found that hyperoxia exposure in neonatal rats caused sustained reductions in lung VEGF expression and persistent abnormalities in lung structure, including decreased vascular growth and impaired alveolarization. We also report that treatment with low doses of inhaled NO after neonatal hyperoxia enhanced late lung growth and improved alveolarization during the recovery period. Further studies are needed to determine the exact mechanisms by which inhaled NO improves lung structure after neonatal hyperoxia, but these findings suggest that inhaled NO therapy may play a therapeutic role in enhancing distal lung growth in BPD.

REFERENCES

- Northway WH Jr, Rosan RC, Porter DY 1967 Pulmonary disease following respiratory therapy of hyaline-membrane disease. Bronchopulmonary dysplasia. *N Engl J Med* 276:357–368
- Husain AN, Siddiqui NH, Stocker JT 1998 Pathology of arrested acinar development in postsurfactant bronchopulmonary dysplasia. *Hum Pathol* 29:710–717
- Jobe AH, Bancalari E 2001 Bronchopulmonary dysplasia. *Am J Respir Crit Care Med* 163:1723–1729
- Abman SH 2001 Bronchopulmonary dysplasia: “a vascular hypothesis.” *Am J Respir Crit Care Med* 164:1755–1756
- Bhatt AJ, Pryhuber GS, Huyck H, Watkins RH, Metlay LA, Maniscalco WM 2001 Disrupted pulmonary vasculature and decreased vascular endothelial growth factor, Flt-1, and TIE-2 in human infants dying with bronchopulmonary dysplasia. *Am J Respir Crit Care Med* 164:1971–1980
- Lassus P, Turanlahti M, Heikkilä P, Andersson LC, Nupponen I, Sarnesto A, Andersson S 2001 Pulmonary vascular endothelial growth factor and Flt-1 in fetuses, in acute and chronic lung disease, and in persistent pulmonary hypertension of the newborn. *Am J Respir Crit Care Med* 164:1981–1987
- Jakkula M, Le Cras TD, Gebb S, Hirth KP, Tudor RM, Voelkel NF, Abman SH 2000 Inhibition of angiogenesis decreases alveolarization in the developing rat lung. *Am J Physiol Lung Cell Mol Physiol* 279:L600–L607
- Le Cras TD, Markham NE, Tudor RM, Voelkel NF, Abman SH 2002 Treatment of newborn rats with a VEGF receptor inhibitor causes pulmonary hypertension and abnormal lung structure. *Am J Physiol Lung Cell Mol Physiol* 283:L555–L562
- Le Cras TD, Tyler RC, Horan MP, Morris KG, McMurty IF, Johns RA, Abman SH 1998 Effects of chronic hypoxia and altered hemodynamics on endothelial nitric oxide synthase and preendothelin-1 expression in the adult rat lung. *Chest* 114:S35–S36
- Roberts RJ, Weesner KM, Bucher JR 1983 Oxygen-induced alterations in lung vascular development in the newborn rat. *Pediatr Res* 17:368–375
- Warner BB, Stuart LA, Papes RA, Wispe JR 1998 Functional and pathological effects of prolonged hyperoxia in neonatal mice. *Am J Physiol Lung Cell Mol Physiol* 275:L110–L117
- Wilson WL, Mullen M, Olley PM, Rabinovitch M 1985 Hyperoxia-induced pulmonary vascular and lung abnormalities in young rats and potential for recovery. *Pediatr Res* 19:1059–1067
- Klekamp JG, Jarzecka K, Perrett EA 1999 Exposure to hyperoxia decreases the expression of vascular endothelial growth factor and its receptors in adult rat lungs. *Am J Pathol* 154:823–831
- Maniscalco WM, Watkins RH, Finkelstein JN, Campbell MH 1995 Vascular endothelial growth factor mRNA increases in alveolar epithelial cells during recovery from oxygen injury. *Am J Respir Cell Mol Biol* 13:377–386
- Maniscalco WM, Watkins RH, Pryhuber GS, Bhatt A, Shea C, Huyck H 2002 Angiogenic factors and alveolar vasculature: development and alterations by injury in very premature baboons. *Am J Physiol Lung Cell Mol Physiol* 282:L811–L823
- Kroll J, Waltenberger J 1999 A novel function of VEGF receptor-2 (KDR): rapid release of nitric oxide in response to VEGF-A stimulation in endothelial cells. *Biochem Biophys Res Commun* 265:636–639
- Papapetropoulos A, Garcia-Cardena G, Madri JA, Sessa WC 1997 Nitric oxide production contributes to the angiogenic properties of vascular endothelial growth factor in human endothelial cells. *J Clin Invest* 100:3131–3139
- Schreiber MD, Gin-Mesten K, Marks JD, Huo D, Lee G, Srissuparp P 2003 Inhaled nitric oxide in premature infants with respiratory distress syndrome. *N Engl J Med* 349:2099–107
- Han RN, Babaei S, Robb M, Lee T, Ridsdale R, Ackerley C, Post M, Stewart DJ 2004 Defective lung vascular development and fatal respiratory distress in endothelial NO synthase deficient mice: a model of alveolar capillary dysplasia? *Circ Res* 94:1115–1123
- Balasubramaniam V, Tang JR, Maxey A, Plopper CG, Abman SH 2003 Mild hypoxia impairs alveolarization in the endothelial nitric oxide synthase-deficient mouse. *Am J Physiol Lung Cell Mol Physiol* 284:L964–L971
- Gutierrez HH, Nieves B, Chumley P, Rivera A, Freeman BA 1996 Nitric oxide regulation of superoxide-dependent lung injury: oxidant-protective actions of endogenously produced and exogenously administered nitric oxide. *Free Radic Biol Med* 21:43–52
- Howlett CE, Hutchison JS, Veinot JP, Chiu A, Merchant P, Fliss H 1999 Inhaled nitric oxide protects against hyperoxia-induced apoptosis in rat lungs. *Am J Physiol* 277:L596–L605
- McElroy MC, Wiener-Kronish JP, Miyazaki H, Sawa T, Modelska K, Dobbs LG, Pittet JF 1997 Nitric oxide attenuates lung endothelial injury caused by sublethal hyperoxia in rats. *Am J Physiol* 272:L631–L638
- Nelin LD, Welty SE, Morrisey JF, Gotuaco C, Dawson CA 1998 Nitric oxide increases the survival of rats with a high oxygen exposure. *Pediatr Res* 43:727–732
- Cooney TP, Thurlbeck WM 1982 The radial alveolar count method of Emery and Mithal: a reappraisal 1—postnatal lung growth. *Thorax* 37:572–579
- Cooney TP, Thurlbeck WM 1982 The radial alveolar count method of Emery and Mithal: a reappraisal 2—intrauterine and early postnatal lung growth. *Thorax* 37:580–583
- Meyrick B, Reid LM 1978 The effect of continued hypoxia on the rat pulmonary circulation. An ultrastructural study. *Lab Invest* 38:188–200
- Tang JR, Markham NE, Lin YJ, McMurty IF, Maxey A, Kinsella JP, Abman SH 2004 Inhaled nitric oxide attenuates pulmonary hypertension and improves lung growth in infant rats after neonatal treatment with a VEGF receptor inhibitor. *Am J Physiol Lung Cell Mol Physiol* 287:L344–L351
- Deleted in proof
- Maniscalco WM, Watkins RH, D'Angio CT, Ryan RM 1997 Hyperoxic injury decreases alveolar epithelial cell expression of vascular endothelial growth factor (VEGF) in neonatal rabbit lung. *Am J Respir Cell Mol Biol* 16:557–567
- Hosford GE, Olson DM 2003 Effects of hyperoxia on VEGF, its receptors, and HIF-2 α in the newborn rat lung. *Am J Physiol Lung Cell Mol Physiol* 285:L161–L168
- Leuwerke SM, Kaza AK, Tribble CG, Kron IL, Laubach VE 2002 Inhibition of compensatory lung growth in endothelial nitric oxide synthase-deficient mice. *Am J Physiol Lung Cell Mol Physiol* 282:L1272–L1278
- Young SL, Evans K, Eu JP 2002 Nitric oxide modulates branching morphogenesis in fetal rat lung explants. *Am J Physiol Lung Cell Mol Physiol* 282:L379–L385
- Afshar S, Gibson LL, Yuhanna IS, Sherman TS, Kerecman JD, Grubb PH, Yoder BA, McCurnin DC, Shaul PW 2003 Pulmonary NO synthase expression is attenuated in a fetal baboon model of chronic lung disease. *Am J Physiol Lung Cell Mol Physiol* 284:L749–L758
- MacRitchie AN, Albertine KH, Sun J, Lei PS, Jensen SC, Freestone AA, Clair PM, Dahl MJ, Godfrey EA, Carlton DP, Bland RD 2001 Reduced endothelial nitric oxide synthase in lungs of chronically ventilated preterm lambs. *Am J Physiol Lung Cell Mol Physiol* 281:L1011–L1020
- Gries DM, Tam EK, Blaisdell JM, Iwamoto LM, Fujiwara N, Ueyehara CF, Nakamura KT 2000 Differential effects of inhaled nitric oxide and hyperoxia on pulmonary dysfunction in newborn guinea pigs. *Am J Physiol Regul Integr Comp Physiol* 279:R1525–R1530
- Issa A, Lappalainen U, Kleinman M, Bry K, Hallman M 1999 Inhaled nitric oxide decreases hyperoxia-induced surfactant abnormality in preterm rabbits. *Pediatr Res* 45:247–254
- Turanlahti M, Pesonen E, Lassus P, Andersson S 2000 Nitric oxide and hyperoxia in oxidative lung injury. *Acta Paediatr* 89:966–970

39. Ekekezie II, Thibeault DW, Rezaiekhalthigh MH, Mabry SM, Norberg M, Reddy GK, Youssef J, Truog WE 2000 High-dose inhaled nitric oxide and hyperoxia increases lung collagen accumulation in piglets. *Biol Neonate* 78:198–206
40. Ekekezie II, Thibeault DW, Zwick DL, Rezaiekhalthigh MH, Mabry SM, Morgan RE, Norberg M, Truog WE 2000 Independent and combined effects of prolonged inhaled nitric oxide and oxygen on lung inflammation in newborn piglets. *Biol Neonate* 77:37–44
41. Lightfoot RT, Khov S, Ischiropoulos H 2004 Transient injury to rat lung mitochondrial DNA following exposure to hyperoxia and inhaled nitric oxide. *Am J Physiol Lung Cell Mol Physiol* 286:L23–L29
42. Storme L, Riou Y, Dubois A, Fialdes P, Jaillard S, Klosowski S, Dupuis B, Lequien P 1999 Combined effects of inhaled nitric oxide and hyperoxia on pulmonary vascular permeability and lung mechanics. *Crit Care Med* 27:1168–1174
43. Youssef JA, Thibeault DW, Rezaiekhalthigh MH, Mabry SM, Norberg MI, Truog WE 1999 Influence of inhaled nitric oxide and hyperoxia on Na,K-ATPase expression and lung edema in newborn piglets. *Biol Neonate* 75:199–209
44. Ferrara N, Gerber HP, LeCouter J 2003 The biology of VEGF and its receptors. *Nat Med* 9:669–676
45. Massaro D, Teich N, Maxwell S, Massaro GD, Whitney P 1985 Postnatal development of alveoli. Regulation and evidence for a critical period in rats. *J Clin Invest* 76:1297–1305
46. Chen Y, Whitney PL, Frank L 1994 Comparative responses of premature versus full-term newborn rats to prolonged hyperoxia. *Pediatr Res* 35:233–237
47. Bucher JR, Roberts RJ 1981 The development of the newborn rat lung in hyperoxia: a dose-response study of lung growth, maturation, and changes in antioxidant enzyme activities. *Pediatr Res* 15:999–1008
48. Levine CR, Kazzaz JA, Koo HC, Chester D, Merritt TA, Matalon S, Pollack S, Davis JM 2002 Effects of variable concentrations of inhaled nitric oxide and oxygen on the lungs of newborn piglets. *Pediatr Pulmonol* 34:58–65
49. Robbins CG, Horowitz S, Merritt TA, Kheiter A, Tierney J, Narula P, Davis JM 1997 Recombinant human superoxide dismutase reduces lung injury caused by inhaled nitric oxide and hyperoxia. *Am J Physiol* 272:L903–L907